Joint Fading and Doppler Shift Estimation for Underwater Acoustic MISO Communication System

Junfeng Wang, Yue Cui, Zeyad A. H. Qasem, Miaowen Wen, *Senior Member, IEEE*, Jianghui Li, and Haixin Sun, *Senior Member, IEEE*

***Abstract*—The fading of underwater channels and Doppler shifts are two major challenges in underwater acoustic multiple-input single-output (MISO) communication systems, significantly degrading performance. To address these challenges, this letter proposes a joint fading and Doppler shift estimation scheme for underwater acoustic MISO system. We begin by deriving a composite fading coefficient, which encapsulates both propagation and absorption loss effects. Building on this coefficient, we develop maximum likelihood and autocorrelation-based Doppler estimators. We then evaluate the proposed scheme under various scenarios through computer simulations, comparing its performance to classical algorithms and theoretical Cramér–Rao bounds. The results demonstrate that our proposed approach outperforms existing techniques and closely approaches the theoretical limits, thus confirming its effectiveness in underwater acoustic MISO communication.**

***Index Terms*—Underwater acoustic communications, MISO, doppler shift, composite fading coefficient, Cramér-Rao bounds.**

I. Introduction

UNDERWATER acoustic communications have attracted significant attention in applications ranging from fundamental missions to extensive research in marine biology, given that underwater radio and optical waves have limited ranges, and cables are heavier and more expensive than wireless media [1], [2], [3], [4]. Moreover, in contrast to the radio or optical wave propagation environments, dynamic features of oceans such as tidal, seasonal, and diurnal cycles lead to a more complex underwater channels. In order to improve the communication performance of the underwater acoustic system, the multiple-input single-output (MISO) technology employing beamforming boycotts the acoustic multiple path fading loss to enhance the underwater acoustic communication quality.

Underwater environments inherently involve mobility, except for the relative mobility of transceivers. This mobility leads to a Doppler shift at the receiver side, and the relatively low speed of underwater acoustic waves ($\sim$ 1500 m/s) implies that even moderate motion, e.g., transmitter or/and receiver mounted on a surface vessel which is contingent on sea surface waves or/and water currents, or on an autonomous underwater vehicle (AUV) with modest movement, generates a greater Doppler shift than those experienced in radio or optical wave transmission. The Doppler shift is an important factor and is utilized for the localization and tracking system. By contrast, it can result in significant degradation of communication performance for the underwater acoustic communication system [5]. Additionally, for sophisticated propagation characteristics with the exception of underwater acoustic ambient noise, another key aspect that impairs reliable underwater acoustic communication is underwater channel fading. In summary, the estimation of Doppler shift and channel fading plays a considerable role in numerous underwater acoustic communication systems.

To address severe Doppler shift effects, several popular data-assisted methods have been presented to mitigate these issues in the underwater acoustic communication system. These data-assisted approaches rely on the periodic transmission of known blocks. Linear frequency modulated (LFM) signal is generally arranged in known blocks, as it has large time-bandwidth product and low interception characteristics. The existing classical scheme used in Doppler shift estimation employs a group of correlators to compute the correlation values, and selects the maximum one to be utilized as the corresponding Doppler shift estimation [6], [7], [8]. However, as the number of correlators decreases, the estimation performance degrades, and the overall complexity is reduced. Current popular applications of time-frequency (TF) analysis methods such as fractional Fourier transform (FrFT) to Doppler shift estimation of LFM signals appear in [9], [10], which can achieve relatively good results due to its TF local properties. Nevertheless, the computational complexity increases because of the stepwise search required by these methods. Besides, in order to address the issue of channel fading that can be further processed to initiate adaptive transmission conditions, optimal power allocation operation and other applications in

Received 19 October 2025; accepted 25 November 2025. Date of publication 3 December 2025; date of current version 26 December 2025. This work was supported in part by the Stable Supporting Fund of National Key Laboratory of Underwater Acoustic Technology under Grant JCKYS2023604SSJS008; in part by the Key Laboratory of Southeast Coast Marine Information Intelligent Perception and Application, MNR, under Grant 24203; and in part by the National Natural Science Foundation of China under Grant 62201385 and Grant 62271426. The associate editor coordinating the review of this article and approving it for publication was S. P. Herath. *(Corresponding authors: Junfeng Wang; Yue Cui.)*

Junfeng Wang is with the Department of Communication Engineering, Tianjin University of Technology, Tianjin 300384, China (e-mail: great_seal@163.com).

Yue Cui is with the College of Computer and Information Engineering, Tianjin Normal University, Tianjin 300387, China (e-mail: cuiyue_enya@126.com).

Zeyad A. H. Qasem is with the Institute of Intelligent Marine Sensing and Communications, Donghai Laboratory, Zhoushan 316000, China (e-mail: zeyadqasem@zju.edu.cn).

Miaowen Wen is with the School of Electronic and Information Engineering, South China University of Technology, Guangzhou 510640, China (e-mail: eemwwen@scut.edu.cn).

Jianghui Li is with the College of Ocean and Earth Sciences, Xiamen University, Xiamen 361005, China (e-mail: jli@xmu.edu.cn).

Haixin Sun is with the School of Informatics, Xiamen University, Xiamen 361005, China (e-mail: hxsun@xmu.edu.cn).

Digital Object Identifier 10.1109/LWC.2025.3639203

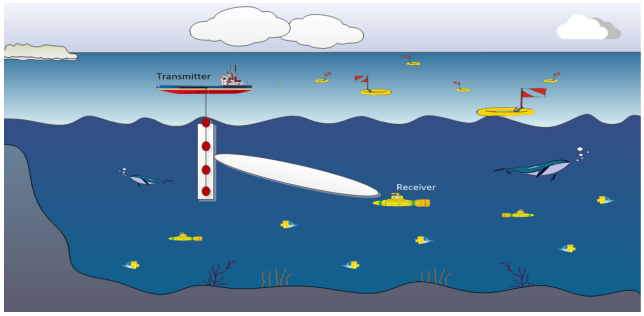

Fig. 1. An illustration of the underwater acoustic MISO communication system.

underwater communications, many classical schemes such as least square (LS) and minimum mean square error have been investigated over decades [11], [12], [13]. Bhadouria and Han studied joint Doppler and channel estimation in [14], [15]. However, their approaches still entail high-dimensional matrix operations and highly complex peak search computations in dense multipath scenarios. Without doubt, beamforming techniques can overcome these difficulties by suppressing multipath propagation [16]. Furthermore, to the best of our knowledge, no existing literature has investigated joint fading and Doppler shift estimation for underwater acoustic MISO communication systems.

To fill this gap, we propose, for the first time, a joint fading and Doppler shift estimation scheme for underwater acoustic MISO communication systems. More specifically, the contributions of this work are summarized as follows: 1) We first derive a composite fading coefficient, based on two lemmas, that provides an unbiased estimate; 2) Using this coefficient, we propose maximum likelihood and autocorrelation-based Doppler shift estimators, which are nearly unbiased; and 3) The performance of the proposed approach is elaborated via numerical simulation to demonstrate its advantages over its benchmarks.

II. System Model

This section describes the system model (see the illustration in Fig. 1), including the transmit signals, the fading channels, and the received signals in an underwater acoustic MISO communication system.

A. Transmit Signals

The frame structure of the transmitted signals used in the underwater acoustic MISO communication system is depicted in Fig. 2. The initialization block is for acquiring the synchronization parameters such as timing and Doppler shift. Assume that the transmitter is equipped with a uniform linear array of N_T transducers, and that the initialization block is with known LFM waveform $x(t)$. In the following, the signal $x(t)$ will be transmitted over array with N_T transducers utilizing a beamforming vector $\mathbf{f}_T$, which is formulated as

$$\tilde{\mathbf{x}}(t) = \mathbf{f}_T x(t), \tag{1}$$

where $\mathbf{f}_T$ is beams steering to the anticipated direction θ, and can be written as

$$\mathbf{f}_T = \sqrt{p_T/N_T}\mathbf{a}(\theta), \tag{2}$$

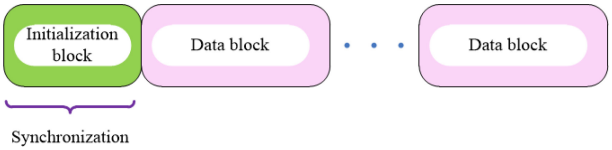

Fig. 2. The frame structure of the transmitted signals used in the system.

where p_T stands for the transmit power allocated to the steering partner, and steering vector $\mathbf{a}(\theta) = [a_1(\theta), \ldots, a_{N_T}(\theta)]^T$.[1] Next, the transmitted signals $\tilde{\mathbf{x}}(t)$ will be through the MISO fading channels that will be introduced in the following section.

B. MISO Channels

In this letter, we consider the receiver to be equipped with a single hydrophone. The MISO fading channels between transceivers have been elaborated, which can be modeled by a principal-path-dominated one with the angle θ,[2] formulating as

$$\mathbf{h}(t) = L_s(d)L_a(d)\mathbf{a}^H(\theta)exp(j2\pi f_D t), \tag{3}$$

where f_D represents the Doppler shift, $(\cdot)^H$ denotes the Hermitian transpose operation, $L_s(d)$ is propagation loss (spreading loss) coefficient that can be expressed by

$$L_s(d) = \frac{1}{d^{\alpha/2}}, \tag{4}$$

where d represents the propagation distance (in meters), α is the spreading factor, and $L_a(d)$ is the absorption loss coefficient that can be written as

$$L_a(d) = 10^{-[(\frac{d}{1000})\beta]/20}, \tag{5}$$

where β is absorption factor (in dB/km) detailed in [18].

C. Received Signals

The received signals at the receiver are given by

$$y(t) = Lexp(j2\pi f_D t)\ \mathbf{a}^H(\theta)\tilde{\mathbf{x}}(t) + w(t), \tag{6}$$

where $L = L_s(d)L_a(d)$ is the composite fading coefficient, and $w(t)$ is the additional white Gaussian noise with variance σ^2. By substituting (1) in (6), we obtain a new expression for the sampled version of the received signals after timing synchronization as

$$\begin{aligned} y(n) &= L\sqrt{p_T N_T}exp(j2\pi f_D n)\ x(n) + w(n) \\ &= \bar{L}exp(j2\pi f_D n)\ x(n) + w(n), \end{aligned} \tag{7}$$

where $\bar{L} = L\sqrt{p_T N_T}$.

[1] $(\cdot)^T$ represents transpose operation. Also, the anticipated direction θ is assumed as the one of principal path and has *a priori* information according to feedback link.

[2] Beamforming toward the principal path is indeed a credible approach [17]. In our work, we consider the pointed beam in the principal-path-dominated direction θ at the transmitter and, therefore, consider principal-path-dominated fading channels only. However, imperfect link considerations, such as the angle difference between the feedback link and the perfect link of transceivers, are possible for some practical scenarios, which can be addressed through angle prediction methods and is out of the scope of this letter.

III. Proposed Scheme

This section proposes a joint fading and Doppler shift estimation scheme for the underwater acoustic MISO communication system. From (7), we observe that L is an unknown composite fading coefficient, which must be determined before estimating the Doppler shift. Next, we present two lemmas on the second- and fourth-order statistics of $y(n)$, i.e.,

Lemma 1: The second-order statistic of $y(n)$ can be written as

$$\begin{aligned} R_{yy}(m) &\triangleq E\{y^*(n)\cdot y(n+m)\} \\ &= \bar{L}^2 exp(j2\pi f_D m)\, x^*(n)x(n+m) + \sigma^2\delta(m), \end{aligned} \tag{8}$$

where $E\{\cdot\}$ stands for the statistical average operator, $(\cdot)^*$ represents conjugate operation, $\delta(\cdot)$ denotes the Kronecker delta function, and

Lemma 2: the fourth-order statistic of $y(n)$ can be expressed as

$$\begin{aligned} &R_{yyyy}(o,m,q) \\ &\triangleq E\big\{y^*(n)\cdot y(n+o)\ \cdot y(n+m)\ \cdot y^*(n+q)\ \big\} \\ &= \bar{L}^4 exp\Big(j2\pi f_D(o+m-q)\Big) \\ &\cdot x^*(n)x(n+o)\ x(n+m)\ x^*(n+q) \\ &+ \bar{L}^2 exp(j2\pi f_D o)x^*(n)x(n+o)\ \sigma^2\delta(m-q) \\ &+ \bar{L}^2 exp(j2\pi f_D m)x^*(n)x(n+m)\ \sigma^2\delta(o-q) \\ &+ \bar{L}^2 exp\Big(j2\pi f_D(o-q)\Big)x(n+o)\ x^*(n+q)\ \sigma^2\delta(m) \\ &+ \bar{L}^2 exp\Big(j2\pi f_D(m-q)\Big)x(n+m)\ x^*(n+q)\ \sigma^2\delta(o) \\ &+ \sigma^4\Big(\delta(o)\delta(m-q)+\delta(m)\delta(o-q)\Big). \end{aligned} \tag{9}$$

Proof: In the Lemma 1 and Lemma 2, we assume that $x(\cdot)$ is independent of $w(\cdot)$.

For Lemma 1, in addition to the aforementioned assumptions, using identity $E\{w^*(k)w(k+m)\}\equiv\sigma^2\delta(m)$, inserting (7) into the definition of (8), i.e., $R_{yy}(m)\triangleq E\{y^*(n)\cdot y(n+m)\}$, and performing some mathematical operations, Equation (8) can be obtained.

For Lemma 2, the fundamental identities, such as $E\{(w(k+m)w(k+o))^*\}\equiv 0$, $E\{w(k+m)w(k+o)\}\equiv 0$, $E\{w^*(k)w(k+m)w(k+o)\}\equiv 0$, $E\{w(k+o)w(k+m)w^*(k+q)\}\equiv 0$, $E\{w^*(k)w(k+m)w^*(k+q)\}\equiv 0$, $E\{w^*(k)w(k+o)w^*(k+q)\}\equiv 0$, and $E\{w^*(k)w(k+o)w(k+m)w^*(k+q)\}\equiv E\{w^*(k)w(k+o)\}E\{w(k+m)w^*(k+q)\}+E\{w^*(k)w(k+m)\}E\{w(k+o)w^*(k+q)\}$, are employed for the derivation of (9).

Similarly to the proof procedure of Lemma 1, substituting (7) into the definition of (9), namely, $R_{yyyy}(o,m,q)\triangleq E\{y^*(n)\cdot y(n+o)\ \cdot y(n+m)\ \cdot y^*(n+q)\ \}$, upon employing the fundamental identities mentioned above and doing some mathematical operations, we have Equation (9).

The detailed derivations of (8) and (9) are lengthy and have been omitted for the sake of brevity. ■

Employing Lemma 1 and Lemma 2, the following proposition on the composite fading coefficient and Doppler shift estimators is presented.

Proposition 1: The estimation of the composite fading coefficient for the underwater acoustic MISO communication system can be given by

$$\hat{L} = \Big(2\hat{R}_{yy}^2(0) - \hat{R}_{yyyy}(0,0,0)\ \Big)^{\frac{1}{4}}/\sqrt{p_T N_T}. \tag{10}$$

Using this composite fading coefficient, we propose two approaches, one maximum likelihood (ML) based and one autocorrelation (AC) based, to infer the Doppler shift. A maximum likelihood scheme for Doppler shift estimation is presented as follows

$$\hat{f}_D^{ML} = \arg\min_{f_D\in\mathcal{D}} |y(n) - \hat{\bar{L}} exp(j2\pi f_D n)\ x(n)|^2, \tag{11}$$

where $\mathcal{D}$ stands for the set of the Doppler shift, and $\hat{\bar{L}} = \hat{L}\sqrt{p_T N_T}$. In addition, an autocorrelation-based Doppler shift estimator is proposed below

$$\begin{aligned} &\hat{f}_D^{AC} = \\ &\frac{1}{2\pi m}\arg\Big\{E\{(y(n)x^*(n))^*\cdot(y(n+m)x^*(n+m))\}/\hat{\bar{L}}^2\Big\}, \end{aligned} \tag{12}$$

where $\arg\{\cdot\}$ denotes phase extracting operation. In order to further improve its performance, employing difference method to (12) can obtain an accurate solution, following

$$\begin{aligned} &\hat{f}_D^{AC} = \frac{1}{2\pi M} \\ &\sum_{m=1}^{M}\Big\{\arg\Big\{E\{(y(n)x^*(n))^*(y(n+m)x^*(n+m))\}/\hat{\bar{L}}^2\Big\} - \\ &\arg\Big\{E\{(y(n)x^*(n))^*(y(n+m-1)x^*(n+m-1))\}/\hat{\bar{L}}^2\Big\}\Big\}. \end{aligned} \tag{13}$$

Proof: From (8) and (9), we observe that $\bar{L}$ and σ appear in these equations alongside the Doppler term. Thus, we can perform algebraic manipulations on (8) and (9) to deduce $\bar{L}$. In the following proof, this assumption has been used: $x^*(\cdot)x(\cdot)=1$. Let $o=m=q=0$ in the Lemma 2, formulating as

$$R_{yyyy}(0,0,0)\ = -\bar{L}^4 + 2\Big(\bar{L}^2+\sigma^2\Big)^2. \tag{14}$$

Let $m=0$ in the Lemma 1, we can obtain

$$R_{yy}(0) = \bar{L}^2 + \sigma^2. \tag{15}$$

Inserting (15) in (14), it can be obtained as

$$\bar{L}^4 = 2R_{yy}^2(0) - R_{yyyy}(0,0,0). \tag{16}$$

Let $\hat{R}_{yyyy}(\cdot,\cdot,\cdot)$ and $\hat{R}_{yy}(\cdot)$ be the unbiased estimation of $R_{yyyy}(\cdot,\cdot,\cdot)$ and $R_{yy}(\cdot)$, respectively. Substituting these estimates into (16) yields (10), which we use for the subsequent Doppler shift estimation. The derivation of (11) and (12) is straightforward, and we thus skip for brevity. ■

The aforementioned work shows the proposed fading and Doppler shift estimation scheme. In what follows, we present another proposition for lower bounds (the Cramér-Rao bound is generally utilized for this lower bound [19]) on the suggested composite fading coefficient and Doppler shift estimators.

Proposition 2: The Cramér-Rao bounds on the suggested composite fading coefficient and Doppler shift estimators are

$$\mathrm{CRB}_L = \frac{\sigma^2}{2p_T N_T\sum_n |x(n)|^2}, \tag{17}$$

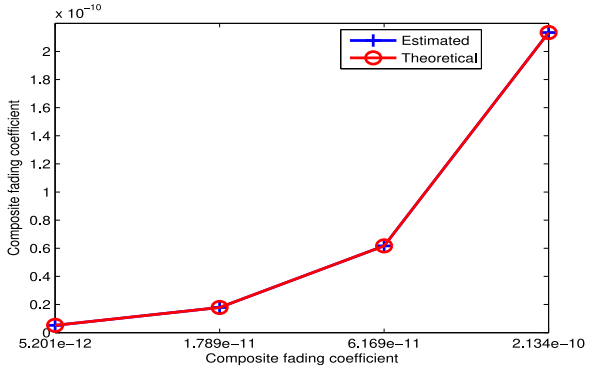

Fig. 3. The estimated composite fading coefficient versus the theoretical one.

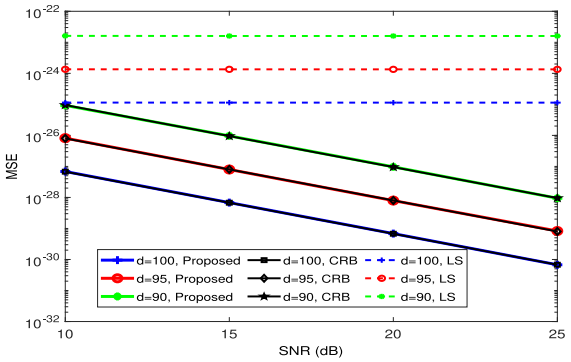

Fig. 4. The MSE versus the SNR for different propagation distances.

and

$$\mathrm{CRB}_{f_D} = \frac{\sigma^2}{8\pi^2 \bar{L}^2 \sum_n n^2 |x(n)|^2}. \tag{18}$$

Proof: For the unknown deterministic composite fading coefficient L and the unknown deterministic Doppler shift f_D in the received signal model, we first collect them into the vector $\xi = (L, f_D)$, and then calculate their Cramér-Rao bounds. According to [19], the (ι, κ)-th element of the Fisher information matrix (FIM) can be given as

$$\begin{aligned}\mathbf{I}(\xi)_{\iota,\kappa} &= -E\left[\frac{\partial^2 \ln p(y(n);\xi)}{\partial \xi_\iota \partial \xi_\kappa}\right] \\ &= \frac{2}{\sigma^2}\mathrm{Re}\left[\sum_n \frac{\partial s^*(n)}{\partial \xi_\iota}\frac{\partial s(n)}{\partial \xi_\kappa}\right],\end{aligned} \tag{19}$$

where $\ln(\cdot)$ is the logarithm operation, $p(y(n);\xi)$ is the probability density function of $y(n)$ for a given ξ, $\mathrm{Re}(\cdot)$ is real operation, and $s(n) = \bar{L} exp(j2\pi f_D n)\ x(n) = L\sqrt{p_T N_T} exp(j2\pi f_D n)\ x(n)$.

Inserting $s(n)$ into (19) and doing some mathematical operations, the entries of the FIM can be expressed as

$$[\mathbf{I}(\xi)]_{1,1} = \frac{2 p_T N_T \sum_n |x(n)|^2}{\sigma^2}, \tag{20}$$

$$[\mathbf{I}(\xi)]_{2,2} = \frac{8\pi^2 \bar{L}^2 \sum_n n^2 |x(n)|^2}{\sigma^2}, \tag{21}$$

and

$$[\mathbf{I}(\xi)]_{1,2} = [\mathbf{I}(\xi)]_{2,1} = 0. \tag{22}$$

Based on Equations (20) to (22), the Cramér-Rao bounds on the presented composite fading coefficient and Doppler shift estimators are given by $\mathrm{CRB}_L = [\mathbf{I}(\xi)]^{-1}_{1,1}$ and $\mathrm{CRB}_{f_D} = [\mathbf{I}(\xi)]^{-1}_{2,2}$, respectively. ■

Alongside theoretical results, we draw attention to the superior performance of our proposed scheme verified via computer simulation in the following section.

IV. Simulation Results

The performance of our proposed scheme is evaluated and compared against the existed benchmarks and the Cramér-Rao bounds. The detailed parameters for α, β and single LFM signal utilized in the test cases are as follows: the spreading factor is $\alpha = 2$, the carrier frequency is $f_c = 10$ kHz, the water depth is 50 meters, $A = 2.34 \times 10^{-6}$, $B = 3.38 \times 10^{-6}$, the salinity is $S_a = 0.035$, the relaxation frequency is $f_T = 1.42$ kHz, the modulation slope is set to 5×10^5, the bandwidth is 5 kHz, the length of the initialization block is 400, and the signal sampling rate is set as 8 times of this bandwidth. In addition, the number of the transducer N_T is set to 6, and $\sqrt{p_T N_T} = 10$.

In the first two simulations, we compare (i) the estimated composite fading coefficient to its theoretical counterpart, and (ii) the mean squared error (MSE) of the estimated coefficient versus the signal-to-noise ratio (SNR). Fig. 3 shows the estimated composite fading coefficient versus the theoretical one, where d is set to 100, 95, 90, as well as 85 meters, f_D is set to 20 Hz,[3] and the SNR is set to 30 dB. Fig. 4 portrays the MSE performance of our suggested scheme, where d ranges from 100 to 90 meters with a step size of 5, f_D is the same as the above setting, and the SNR ranges from 10 to 25 dBs with an equal step size. The LS-based scheme and the Cramér-Rao bound are employed for comparison. From Figs. 3 and 4, we observe that our composite fading coefficient estimator is unbiased, closely matching its Cramér–Rao bound.

In the following simulations, we analyze the performance of the proposed Doppler shift estimators, where d is set to 100 meters. Fig. 5 depicts the estimated Doppler shift versus the theoretical one with SNR = 30dB and Doppler shift ranging from -20 Hz to 20 Hz, where "-" denotes the receiver moving away from the transmitter. As seen from Fig. 5 that our presented estimator is almost unbiased. Fig. 6 illustrates the root MSE (RMSE) of the estimated Doppler shift versus the SNR, where $f_D = 16$ Hz, 10 Hz, as well as 5 Hz, and the SNR is ranging from 10 dB to 25 dB with the equal step size. The revised FrFT-based method and the Cramér-Rao bound are used for performance comparison. From Fig. 6, we observe that the RMSE using the estimated composite fading coefficient matches the theoretical value, demonstrating the benefits of our proposed scheme. Furthermore, Fig. 6 shows that the performance stays close to the Cramér–Rao bound as

[3]As far as we know, the trade-off between the cruise velocity and endurance of the AUVs should generally be considered [20], [21]. The cruise speed is typically set to $3 \sim 5$ knots [20]. The Doppler shift of 20 Hz arranged in this letter corresponds to a velocity of about 6 knot, which enlarges the bounds mentioned above a little, and may be the cruise velocity met in the next generation of the AUVs. Fortunately, the proposed scheme can yield pretty good performance in these velocity values.

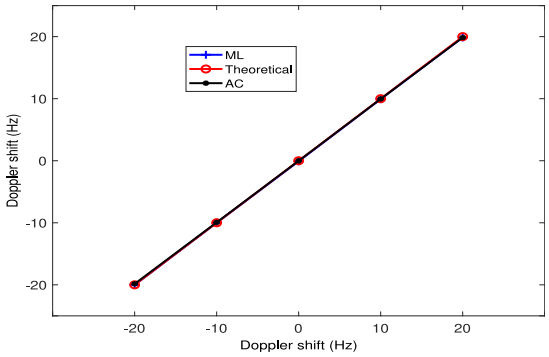

Fig. 5. The estimated Doppler shift versus the theoretical one.

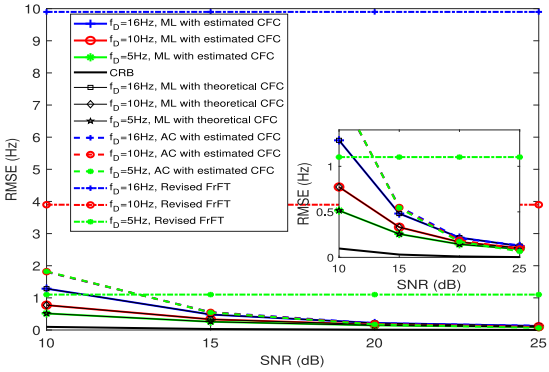

Fig. 6. The RMSE versus the SNR for different f_D with the estimated composite fading coefficient (CFC) and the theoretical one.

the SNR increases. The RMSE of our approach deviates by only 1.36% to 2.87% at 20 dB, thus offering accurate Doppler information for numerous underwater missions.

V. Conclusion

This letter proposes a novel fading and Doppler shift estimation scheme for the underwater acoustic MISO communication system. Initially, we derive an unbiased estimator of the composite fading coefficient using two lemmas on the received signals. Then, by using this estimated coefficient, we perform Doppler shift estimation via maximum likelihood and autocorrelation methods. The simulation results validate the performance predicted by our theory and demonstrate the significant benefits of the proposed approach.

References

[1] M. Cheng, Q. Guan, F. Ji, Y. Huang, and T. Q. S. Quek, "Mobile relaying between USV and AUV under FER constraints for underwater data transmission," *IEEE Commun. Lett.*, vol. 27, no. 12, pp. 3429–3433, Dec. 2023.

[2] L. Yan, X. Ma, X. Li, and J. Lu, "Shot interference detection and mitigation for underwater acoustic communication systems," *IEEE Trans. Commun.*, vol. 69, no. 5, pp. 3274–3285, May 2021.

[3] Y. Li, Y. Zhang, H. Zhou, and T. Jiang, "To relay or not to relay: Open distance and optimal deployment for linear underwater acoustic networks," *IEEE Trans. Commun.*, vol. 66, no. 9, pp. 3797–3808, Sep. 2018.

[4] J. Yan, X. Yang, X. Luo, and C. Chen, "Energy-efficient data collection over AUV-assisted underwater acoustic sensor network," *IEEE Syst. J.*, vol. 12, no. 4, pp. 3519–3530, Dec. 2018.

[5] G. Qiao, X. Liu, L. Ma, S. Mazhar, and Y. Zhao, "Residual Doppler effect analysis of the FBMC/OQAM communication system in underwater acoustic channel," *IEEE Commun. Lett.*, vol. 25, no. 9, pp. 3090–3093, Sep. 2021.

[6] R. Wei, X. Ma, S. Zhao, and S. Yan, "Doppler estimation based on dual-HFM signal and speed spectrum scanning," *IEEE Signal Process. Lett.*, vol. 27, pp. 1740–1744, 2020.

[7] L. Ma, H. Jia, S. Liu, and I. U. Khan, "Low-complexity Doppler compensation algorithm for underwater acoustic OFDM systems with nonuniform Doppler shifts," *IEEE Commun. Lett.*, vol. 24, no. 9, pp. 2051–2054, Sep. 2020.

[8] J. Li, T. Y. V. Zakharov, and B. Henson, "Multibranch autocorrelation method for Doppler estimation in underwater acoustic channels," *IEEE J. Ocean. Eng.*, vol. 43, no. 4, pp. 1099–1113, Oct. 2018.

[9] H. Wang, W. Jiang, Q. Hu, Z. Zeng, and Z. Li, "Time-varying channel and intrablock carrier frequency offset estimation for OFDM underwater acoustic communication," *IEEE Sens. J.*, vol. 24, no. 11, pp. 18405–18417, Jun. 2024.

[10] Z. Gong, C. Li, and F. Jiang, "A machine learning-based approach for auto-detection and localization of targets in underwater acoustic array networks," *IEEE Trans. Veh. Technol.*, vol. 69, no. 12, pp. 15857–15866, Dec. 2020.

[11] L. Wan et al., "Adaptive modulation and coding for underwater acoustic OFDM," *IEEE J. Ocean. Eng.*, vol. 40, no. 2, pp. 327–336, Apr. 2015.

[12] Y. Liu, F. Ji, M. Wen, H. Yu, F. Chen, and D. Wan, "Power allocation for OFDM over multi-scale multi-lag channels," *IEEE Trans. Veh. Technol.*, vol. 67, no. 3, pp. 2345–2358, Mar. 2018.

[13] X. Feng, M. Zhou, J. Wang, H. Sun, G. Pan, and M. Wen, "Model-driven deep learning-based estimation for underwater acoustic channels with uncertain sparsity," *IEEE Trans. Wireless Commun.*, vol. 23, no. 6, pp. 5710–5725, Jun. 2024.

[14] V. S. Bhadouria, M. Agrawal, and R. Kumar, "A prefix-based approach for joint Doppler and channel estimation in underwater communication," *Int. J. Commun. Syst.*, vol. 36, no. 18, pp. 1–28, 2023.

[15] J. Han, S. P. Chepuri, and G. Leus, "Joint channel and Doppler estimation for OSDM underwater acoustic communications," *Signal Process.*, vol. 170, May 2020, Art. no. 107446.

[16] M. Zhou, H. Sun, J. Wang, Z. Xie, and X. Feng, "Channel estimation for underwater acoustic OFDM communications: Recent advances," *Recent Patents Eng.*, vol. 19, no. 3, pp. 13–24, 2025.

[17] D. A. Cuji and M. Stojanovic, "Transmit beamforming for underwater acoustic OFDM systems," *IEEE J. Ocean. Eng.*, vol. 49, no. 1, pp. 145–162, Jan. 2024.

[18] L. M. Brekhovskikh and Y. P. Lysanov, *Fundamentals of Ocean Acoustics*, 3rd ed. New York, NY, USA: Springer, 2002.

[19] S. M. Kay, *Fundamentals of Statistical Signal Processing*. Englewood Cliffs, NJ, USA: Prentice-Hall, 1993.

[20] B. Song et al., "Development trend and key technologies of autonomous underwater vehicles," *Chin. J. Ship Res.*, vol. 17, no. 5, pp. 27–44, 2022.

[21] C. R. Teeneti, T. T. Truscott, D. N. Beal, and Z. Pantic, "Review of wireless charging systems for autonomous underwater vehicles," *IEEE J. Ocean. Eng.*, vol. 46, no. 1, pp. 68–87, Jan. 2021.